Polish Journal of Chemical Technology, 18, 3, 10—16, 10.1515/pjct-2016-0042

Removal of Cr(III) ions from salt solution by nanofiltration: experimental and modelling analysis

Anna Kowalik-Klimczak[1, 2*], Mariusz Zalewski[2], Paweł Gierycz[2]

[1]*Institute for Sustainable Technologies – National Research Institute in Radom, Kazimierza Pułaskiego 6/10, 26-600 Radom, Poland*
[2]*Warsaw University of Technology, Faculty of Chemical and Process Engineering, Waryńskiego 1, 00-645 Warsaw, Poland*
[*]*Corresponding author: e-mail: anna.kowalik-klimczak@itee.radom.pl, a.kowalik@ichip.pw.edu.pl*

The aim of this study was experimental and modelling analysis of the nanofiltration process used for the removal of chromium(III) ions from salt solution characterized by low pH. The experimental results were interpreted with Donnan and Steric Partitioning Pore (DSP) model based on the extended Nernst-Planck equation. In this model, one of the main parameters, describing retention of ions by the membrane, is pore dielectric constant. In this work, it was identified for various process pressures and feed compositions. The obtained results showed the satisfactory agreement between the experimental and modelling data. It means that the DSP model may be helpful for the monitoring of nanofiltration process applied for treatment of chromium tannery wastewater.

Keywords: nanofiltration, chromium(III), DSP model, extended Nernst-Planck equation.

INTRODUCTION

Nanofiltration (NF) is a pressure-driven membrane technique, which can be successfully applied for treatment of both water[1–4] and wastewaters[5–12]. According to the literature data[7–9] and our own investigations[12–14], one of the most important and interesting research area of nanofiltration is the removal of chromium(III) ions from salts solution characterized by low pH. The nanofiltration membrane in such processes, according to its properties, becomes non-permeable for multi-charged ions and permeable for one-charged anions and cations[13–14]. That is why, nanofiltration seems to be a promising process allowing for effective and efficient treatment of chromium tannery wastewaters[7–9, 12–14]. However, to predict the productivity and the effectiveness of the separation of ions from examined solutions at low pH it is necessary to elaborate a physical meaning, mathematical model describing this process. Many different theories have been elaborated to explain the ions separation mechanism into nanofiltration membranes[9, 15–25]. After analysing of the literatures data[15–25] we have stated that both theoretical and experimental works concerning the ions separation mechanism into nanofiltration membranes are not still satisfactory and require further actions. Recently the modelling of nanofiltration of salt solution has been widely investigated[15–25]. The mass transfer through the membrane was described by different models such as Kedem-Katchalsky[19, 20] or Spiegler-Kedem[19, 21, 25]. However none of the models used took into consideration a density of membrane surface charge, which, as it was mentioned, is one of the main factors in the case of nanofiltration of salt solutions at low pH[12, 14, 26]. Therefore, the Donnan and Steric Partitioning Pore (DSP) model based on the extended Nernst-Planck equation has been proposed for interpretation of the separation of ions from acid solution on nanofiltration membranes.

The main objective of this work was the experimental and modelling analysis of the nanofiltration used for the removal of chromium(III) and chloride ions from salt solution characterized by low pH.

DSP MODEL DESCRIPTION

The transport of ions inside the membrane can be described by the extended Nernst-Planck equation (1). This equation contains three terms due to contributions from diffusion, electromigration and convection, respectively.

$$J_i = -K_{i,d} D_i \frac{dc_i}{dx} - \frac{z_i c_i K_{i,d} D_i}{RT} F \frac{d\psi}{dx} + K_{i,c} c_i V \tag{1}$$

where J_i is the molar flux of species i [mol m^{-2} s^{-1}], $K_{i,d}$ is the ionic hindrance factor for diffusion [–], $K_{i,c}$ is the ionic hindrance factor for convection [–], D_i is the diffusion coefficient of ion i [m^2 s^{-1}], c_i is the concentration of ion i inside pores of the membrane [mol m^{-3}], x is the axial position within the pore [m], Ψ is the electrical potential of ion inside pores [V], F is the Faraday constant [C mol^{-1}], R is the universal gas constant [J mol^{-1} K^{-1}], T is the temperature [K], V is the solvent velocity [m s^{-1}], z_i is the valence of ion i [–].

Solving this equation requires knowing the boundary conditions at the pore inlet and outlet (2).

$$\frac{c_i}{C_i} = \frac{\gamma_{i,sol}}{\gamma_{i,pore}} \phi_i \exp\left(-\Delta W_i\right) \exp\left(\frac{-z_i F}{RT} \Delta\Psi_D\right) \tag{2}$$

where c_i is the concentration of ion i inside the membrane pores [mol m^{-3}], C_i is the concentration of ion i within the polarization layer [mol m^{-3}], $\gamma_{i,sol}$ is the activity coefficient of ion i in the solution side of the interface [–], $\gamma_{i,pore}$ is the activity coefficient of ion i in the pore side of the interface [–], ϕ_i is the steric partition coefficient of ion i [–], ΔW_i is the Born solvation energy barrier [J], z_i is the valence of ion i [–], F is the Faraday constant [C mol^{-1}], R is the universal gas constant [J mol^{-1} K^{-1}], T is the temperature [K], $\Delta\Psi_D$ is the Donnan potential [V].

The hindered nature of diffusion and convection of the ions inside the membrane can be accounted for the terms $K_{i,d}$ (3) and $K_{i,c}$ (4).

$$K_{i,d} = 1 - 2.30\lambda_i + 1.154\lambda_i^2 + 0.224\lambda_i^3 \tag{3}$$

$$K_{i,c} = (2 - \phi_i)(1 + 0.054\lambda_i - 0.998\lambda_i^2 - 0.441\lambda_i^3) \tag{4}$$

$K_{i,d}$ and $K_{i,c}$ can be expressed as a function of the ratio λ_i (the ion i radius r_i [m] related to the pore radius r_p [m]) – (5) and (6).

$$\phi_i = (1 - \lambda_i)^2 \tag{5}$$

$$\lambda_i = \frac{r_i}{r_p} \tag{6}$$

The solvent velocity within the pore (V) related to the pressure gradient through the pore can be described using the Hagen-Poiseuille expression (7), where the osmotic pressure difference is calculated by Van't Hoff equation (8).

$$V = \frac{r_p^2(\Delta P - \Delta\pi)}{8\eta\Delta x} \tag{7}$$

$$\Delta\pi = RT\sum_{i=1}^{n}(c_{i,w} - c_{i,p}) \tag{8}$$

where V is the solvent velocity [m s^{-1}], r_p is the pore radius [m], ΔP is the applied pressure [bar], $\Delta\pi$ is the osmotic pressure difference [bar], η is the dynamic viscosity [bar s], Δx is the membrane thickness [m], R is the universal gas constant [J mol^{-1} K^{-1}], T is the temperature [K], $c_{i,w}$ is the concentration of ion i in the feed [mol m^{-3}], $c_{i,p}$ is the concentration of ion i in permeate [mol m^{-3}].

The solvation energy barrier ΔW_i (9) represented by a decrease of the effective dielectric constant of the solution in the pores can be described by the Born model.

$$\Delta W_i = \frac{z_i^2 e^2}{8\pi\varepsilon_o k_b T r_i}\left(\frac{1}{\varepsilon_p} - \frac{1}{\varepsilon_b}\right) \tag{9}$$

where ΔW_i is the Born solvation energy barrier [J], z_i is the valence of ion i [–], e is the electron charge [–], $\boldsymbol{\varepsilon}_o$ is the permittivity of free space [–], k_b is the Boltzmann constant [J K^{-1}], T is the temperature [K], r_i is the ion i radius [m], $\boldsymbol{\varepsilon}_p$ is the pore dielectric constant [–], $\boldsymbol{\varepsilon}_b$ is the bulk dielectric constant [–].

The electroneutrality conditions in the bulk solution, inside the membrane and in the permeate solution are given by equations (10), (11) and (12), respectively.

$$\sum_{i=1}^{n} z_i c_i = 0 \tag{10}$$

$$\sum_{i=1}^{n} z_i c_i + X_d = 0 \tag{11}$$

$$\sum_{i=1}^{n} z_i c_{i,p} = 0 \tag{12}$$

where z_i is the valence of ion i [–], c_i is the concentration of ion i inside the membrane pores [mol m^{-3}], X_d is the membrane charge density [mol m^{-3}], $c_{i,p}$ is the concentration of ion i in permeate [mol m^{-3}].

Transport of ions through the membrane can be described by applying a set of proper boundary conditions. The ions rejection is calculated by the Nernst-Planck equation (1) written in the form of concentration and potential gradients. The molar flux of species i can be calculated from the following equation (13).

$$J_i = c_{i,p}V \tag{13}$$

where J_i is the molar flux of species i [mol m^{-2} s^{-1}], $c_{i,p}$ is the concentration of ion i in permeate [mol m^{-3}], V is the solvent velocity [m s^{-1}].

Substituting equation (13) into equation (1) and rearranging it, we get the following expression for the concentration gradient (14).

$$\frac{dc_i}{dx} = \frac{V}{D_i}(K_{i,c}c_i - c_{i,p}) - \frac{z_i c_i}{RT}F\frac{d\Psi}{dx} \tag{14}$$

where c_i is the concentration of ion i inside pores of the membrane [mol m^{-3}], x is the axial position within the pore [m], V is the solvent velocity [m s^{-1}], D_i is the diffusion coefficient of ion i [m^2 s^{-1}], $K_{i,c}$ is the ionic (ion i) hindrance factor for convection [–], $c_{i,p}$ is the concentration of ion i in permeate [mol m^{-3}], z_i is the valence of ion i [–], R is the universal gas constant [J mol^{-1} K^{-1}], T is the temperature [K], F is the Faraday constant [C mol^{-1}], Ψ is the electrical potential of ion inside pores [V].

By applying the conditions expressed in equations (10), (11) and (12) to equation (3) and rearranging it, we get the following expression for the electrical potential gradient (15).

$$\frac{d\Psi}{dx} = \frac{\sum_{i=1}^{n}\frac{z_i V}{D_i}(K_{i,c}c_i - c_{i,p})}{\frac{F}{RT}\sum_{i=1}^{n} z_i^2 c_i} \tag{15}$$

where Ψ is the electrical potential of ion inside the pores [V], x is the axial position within the pore [m], z_i is the valence of ion i [–], V is the solvent velocity [m s^{-1}], D_i is the diffusion coefficient of ion i [m^2 s^{-1}], $K_{i,c}$ is the ionic (ion i) hindrance factor for convection [–], c_i is the concentration of ion i inside the membrane pores [mol m^{-3}], $c_{i,p}$ is the concentration of ion i in permeate [mol m^{-3}], F is the Faraday constant [C mol^{-1}], R is the universal gas constant [J mol^{-1} K^{-1}], T is the temperature [K].

The equations (14) and (15) can be solved with the following the conditions:

at $x = 0 \rightarrow c_i = c_{i,w}$

at $x = \Delta x \rightarrow c_i = c_{i,p}$

where $c_{i,w}$ is the concentration of ion i in feed [mol m^{-3}], $c_{i,p}$ is the concentration of ion i in permeate [mol m^{-3}], x is the axial position within the pore [m], Δx is the membrane thickness [m].

The membranes properties are usually determined by retention of ion i – R_i (16) and permeate flux J_P (17).

$$R_i = \left(1 - \frac{c_{i,p}}{c_{i,w}}\right)\cdot 100\% \tag{16}$$

$$J_P = L_P(\Delta P - \Delta\pi) \tag{17}$$

where R_i is the retention of ion i [%], $c_{i,p}$ is the concentration of ion in permeate [mol m^{-3}], $c_{i,w}$ is the concentration of ion i in the feed [mol m^{-3}], J_p is the permeate flux [m^3 m^{-2} s^{-1}], L_p is the permeability coefficient of membrane [m^3 m^{-2} s^{-1} bar^{-1}], ΔP is the applied pressure [bar], $\Delta\pi$ is the osmotic pressure difference [bar].

The average deviation for retention (AD_R) and permeate flux (AD_P) were determined as follows:

$$AD_R = \frac{1}{N}\sum_{1}^{N}\left|\frac{R_{\exp} - R_{\mathrm{mod}}}{R_{\exp}}\right|\cdot 100\% \tag{18}$$

$$AD_P = \frac{1}{N}\sum_{1}^{N}\left|\frac{J_{P\exp} - J_{P\mathrm{mod}}}{J_{P\exp}}\right|\cdot 100\% \tag{19}$$

where AD_R is the average deviation for retention [%], AD_P is the average deviation for permeate flux [%],

N is the number of experimental data points [–], R_{exp} is the experimental retention [%], R_{mod} is the model retention [%], J_{Pexp} is the experimental permeate flux [m^3 m^{-2} s^{-1}], J_{Pmod} is the model permeate flux [m^3 m^{-2} s^{-1}].

EXPERIMENTAL

The experiments were carried out at laboratory scale in a cross flow cell made of stainless steel operated in batch mode with circulation. The installation was described in previous work[12]. Studies concerned solutions with chromium(III), chloride and sulphate ions concentration specific for tannery wastewaters[12–14].

The investigations have been divided into following parts:

The investigation of influence of pore dielectric constant on the change of permeate and retentate composition after nanofiltration of solution containing 2 g Cr^{3+} dm^{-3}, 10 g Cl^- dm^{-3}, 10 g SO_4^{2-} dm^{-3} and characterized by pH ≈ 4.

The investigation of influence of transmembrane pressure (10–24 bar) on the change of permeate and retentate composition after nanofiltration of solution containing 2 g Cr^{3+} dm^{-3}, 10 g Cl^- dm^{-3}, 10 g SO_4^{2-} dm^{-3} and characterized by pH ≈ 4.

The investigation of influence of feed composition on the change of permeate and retentate composition after nanofiltration. In this part, the concentration of sulfate (0–17 g SO_4^{2-} dm^{-3}) and chloride (5–20 g Cl^- dm^{-3}) ions on the change of permeate and retentate composition after nanofiltration of solution containing 2 g Cr^{3+} dm^{-3} and 10 g Cl^- dm^{-3} or 2 g Cr^{3+} dm^{-3} and 10 g SO_4^{2-} dm^{-3} and characterized by pH ≈ 4 were investigated.

The commercial nanofiltration flat sheet membranes (under symbol DL) with effective area of 0.0155 m^2 provided by GE Osmonics were used in the experiments. The characteristic of tested nanofiltration membrane is presented in Table 1.

After the end of the experiment, samples of permeate and retentate have been collected for determination of the chromium(III) and chloride concentration. The samples of permeate, feed and retentate have been analyzed using the following methods:

– chromium(III) – spectrophotometer NANOCOLOR UV/VIS using 1.5-diphenylcarbazide method with wave length λ = 540 nm[27], the concentration of Cr(III) ions was analyzed after the mineralization of samples, each measurement was repeated three times.

– chlorides – the Mohr titration method[28], each measurement was repeated three times.

The feed solution has been prepared using the following chemicals: $CrCl_3 \cdot 6H_2O$ (Sigma-Aldrich), pure NaCl (Chempur®), pure Na_2SO_4 (Chempur®) and the deionized water. The feed solution was characterized by pH ≈ 4. For initial pH correction the pure HCl (Lachner) was used. The pH was measured by pH-meter (Mettler Toledo SevenEasy).

NUMERICAL PROCEDURE

Transport of ions through the active layer of NF membrane was illustrated in Figure 1. Conducting the model calculations of ions transport through the membrane apart from accepting process conditions such as:

Table 1. Characteristic of nanofiltration membrane used in the experimental and modelling analysis

		Reference
Surface material	Poly(piperazine-amide)	12
Support material	Polysulfone	
Type of membrane	Thin film	
Cut-off [g mol^{-1}]	150–300	
Zeta potential [mV] (pH = 4, t = 25°C)	–14.0	
Isoelectric point (pH)	3.0	
Permeability coefficient 10^{-6} [m^3 m^{-2} s^{-1} bar^{-1}]	2.4	13
pH range	2–11	
Max. temperature [°C]	90	
Max. pressure [bar]	40	
Pore radius [nm]	0.94	29

operating pressure (ΔP) and concentration of the ion in feed ($c_{i,w}$) it was necessary to assume the following parameters: the membrane hydraulic permeability coefficient (L_p), the mean pore radius (r_p), the charge density of the membrane (X_d), diffusion coefficient of ions (D_i) and finally the pore dielectric constant (ε_p).

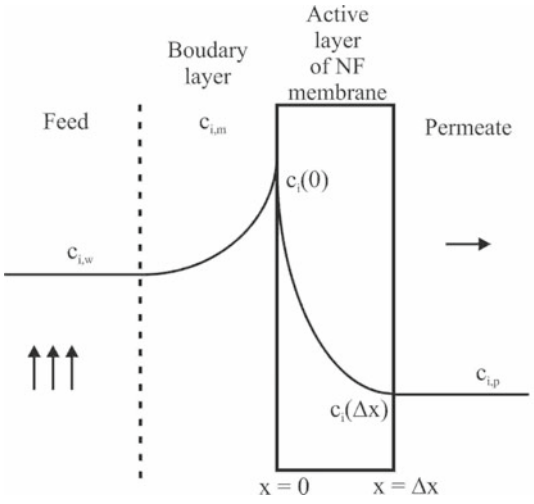

Figure 1. Transport of ions through the active layer of NF membrane

All calculations were performed in open source software for numerical computation Scilab. The concentration of the ions was determined by iteration method shown schematically in Figure 2. As the condition of convergence (CV in Fig. 2) was assumed the smaller than 10^{-6} (five significant digits) change in compositions obtained in one after another iteration. The program has also used the fsolve procedure (modification of the Powell hybrid method) for solving nonlinear equations and the ode procedure (backward differentiation formula method) for solving differential equations. The used equations (Fig. 2) allowed for evaluation of the membranes selectivity determined by the retention (R_i), as well as productivity expressed by the permeate flux (J_P). The properties of the ionic species analyzed in this model listed in Table 2.

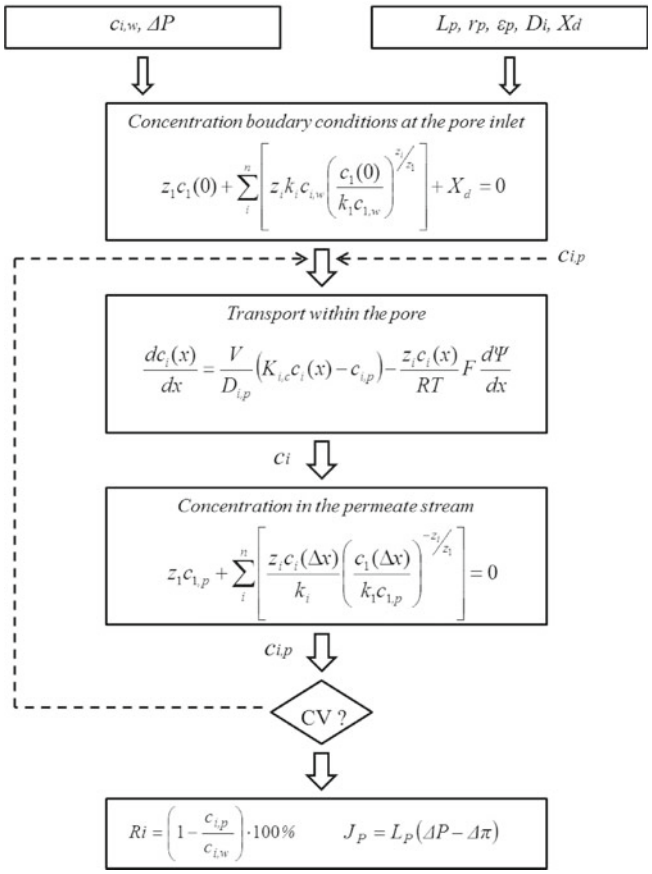

Figure 2. Numerical procedure diagram

Table 2. Properties of the ionic species: M_i – molar mass [g mol^{-1}], r_i – ionic (ion i) radius [m], D_i – diffusion coefficient of ion i [m^2 s^{-1}], zi – valence of ion i [–], [30]

Parameter	Cr^{3+}	Cl^-	SO_4^{2-}
M_i [g mol^{-1}]	52.00	35.45	96.06
r_i [nm]	0.400	0.121	0.231
D_i 10^{-9} [m^2 s^{-1}]	0.062	2.031	1.060
z_i [–]	3	1	2

RESULTS AND DISCUSSION

The influence of pore dielectric constant on the ions transport through NF membrane

The decrease of chromium(III) and chloride ions retention with the increase of pore dielectric constant (ε_p) was observed (Figure 3 and Figure 4). It is due to the fact, that when ions concentration inside the pores increases, the impact of the ions on water molecules is stronger what results in decreasing of dielectric constant. In turn, according to Gomes et al.[9] this phenomenon can be explained by Born solvation energy effect (equation 9). The difference in dielectric constant between external and internal (i.e. inside pores) solutions caused exclusion of both co-ions and counter-ions from membrane pores. Thus, if the pore dielectric constant increases, the Born effect becomes weaker and the salt retention decreases (Figs. 3 and 4). In turn, the low value of the Born energy contributes to the increase in the permeability of small ions, such as Na^+ and Cl^-, present in tested solution. Consequently, the negative retention of chloride ions was observed (Fig. 4). On the basis of these results, the dependence of pore dielectric constant (ε_p) on the process pressure (ΔP) was determined (equation 18).

$$\varepsilon_p = 0.57(\Delta P) + 45 \quad (18)$$

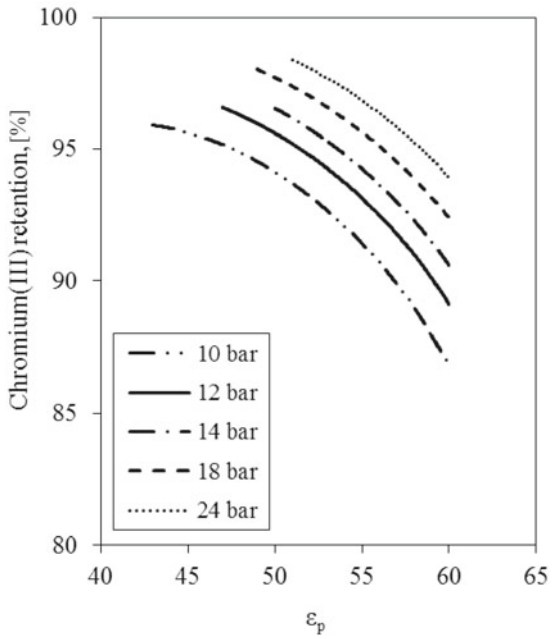

Figure 3. Model retention of chromium(III) ions vs. pore dielectric constant (ε_p) for the feed composition: 2 g Cr^{3+} dm^{-3}, 10 g Cl^- dm^{-3} and 10 g SO_4^{2-} dm^{-3} and ΔP = 10–24 bar

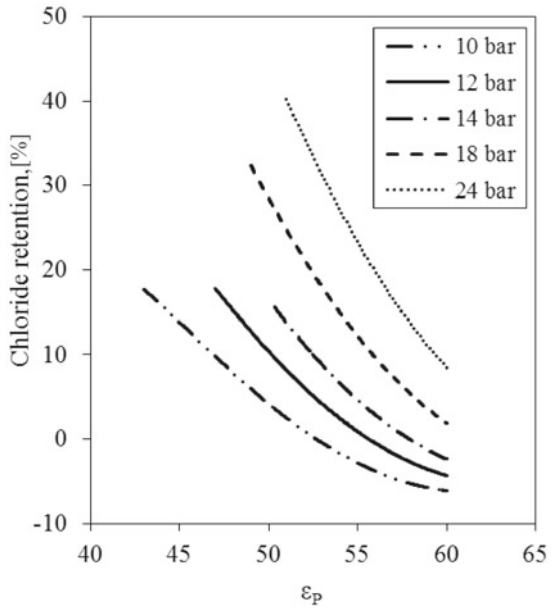

Figure 4. Model retention of chloride ions vs. pore dielectric constant (ε_p) for the feed composition: 2 g Cr^{3+} dm^{-3}, 10 g Cl^- dm^{-3} and 10 g SO_4^{2-} dm^{-3} and ΔP = 10–24 bar

The influence of transmembrane pressure on the ions transport through NF membrane

The use of the equation (18) enabled to obtain a satisfactory agreement between the model data and the experimental results from nanofiltration of chromium(III) salt solutions at acidic pH for ΔP = 10–24 bar both for retention of ions (Fig. 5) and permeate flux (Fig. 6). The average deviations for retention of chromium(III) and chloride ions were equals 1.6% and 5.3%, respectively (Fig. 5), while, the average deviations for permeate flux was equal 1.2% (Fig. 6). The obtained results (Fig. 5) expressed similar relationships: when the process pressure was low the retention tends toward zero, while the process pressure was high retention becomes almost constant. It is caused by the fact that the permeate flux

increases with increasing of the process pressure (Fig. 6), thus the contribution of convective transport becomes more important and retention also increases. This trend is probably opposed by the concentration polarization. Therefore, a constant retention can be achieved with high permeate flux. Similar results have been obtained by Deon et al. for single and mixed salt solutions[17, 18].

The influence of feed composition on the ions transport through NF membrane

The application of the equation (18) for calculation of pore dielectric constant enabled also to obtain a satisfactory agreement between the model data and the experimental results of nanofiltration of chromium(III) acidic solutions containing different concentration of sulphate and chloride ions in the feed (Fig. 7 and 8). The average deviation for retention of chromium(III) and chloride ions were equal to 1.6% and 4.3%, respectively for different concentration of sulphate ions in the feed (Fig. 7a). The average deviations for retention of chromium(III) and chloride ions equal to 1.4% and 5.4%, respectively were obtained for different concentration of chloride ions in the feed (Fig. 7b). It was observed that the increasing of sulphates concentration in the feed caused the decreasing of chlorides retention (Fig. 7a). It was due to a high sulphates concentration, characterized by the negative charge. In these conditions, small chloride ions permeate more quickly and more willingly, according to the Donnan phenomenon. Moreover, when the concentration of Cl^- ions increases, retention of Cl^- ions

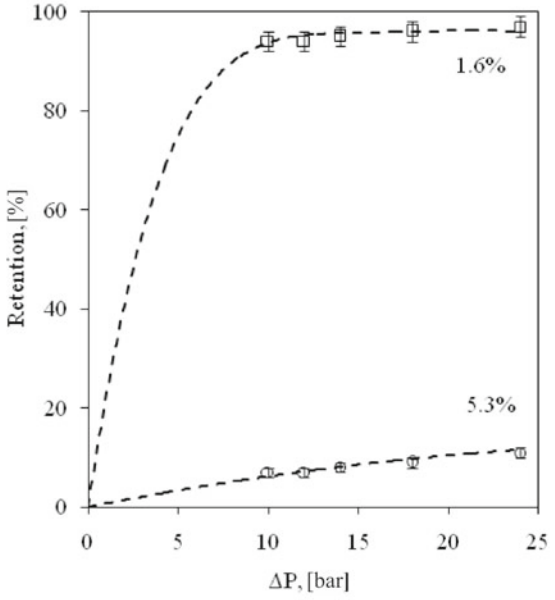

Figure 5. Retention of chromium(III) and chloride ions vs. processes pressure (ΔP) for the feed composition: 2 g Cr^{3+} dm^{-3}, 10 g Cl^- dm^{-3} and 10 g SO_4^{2-} dm^{-3} (□ – chromium(III) retention experimental, ○ – chloride retention experimental, ---- model results)

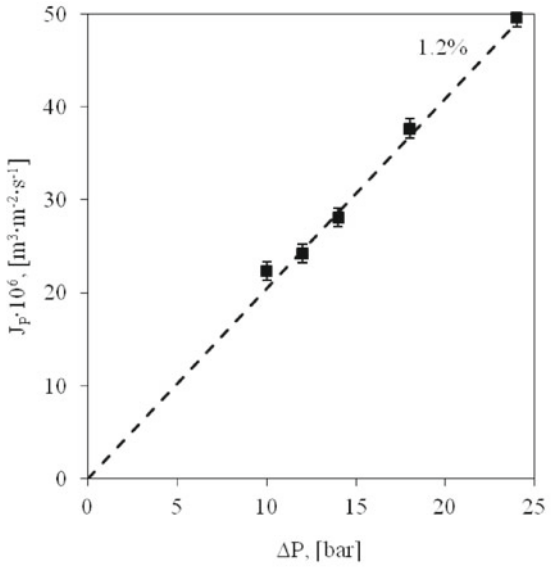

Figure 6. Permeate flux (J_P) vs. processes pressure (ΔP) for the feed composition: 2 g Cr^{3+} dm^{-3}, 10 g Cl^- dm^{-3} and 10 g SO_4^{2-} dm^{-3} (■ – experimental results, ---- model results)

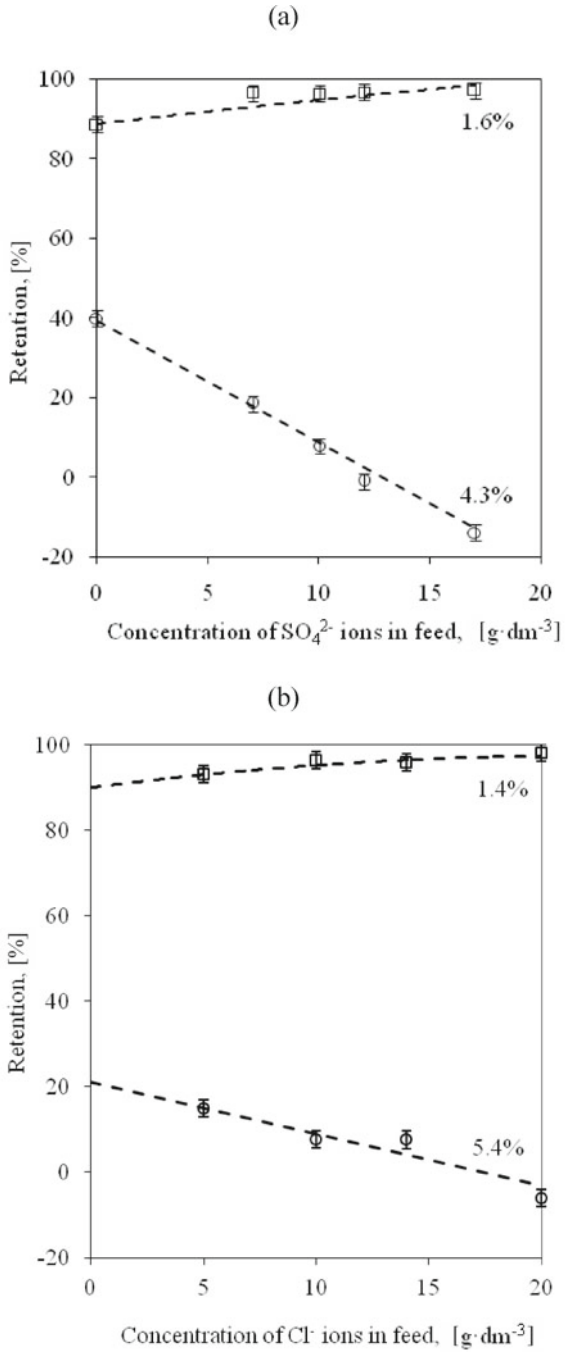

Figure 7. Retention of chromium(III) and chloride ions vs. concentration of sulfate (a) and chloride (b) ions in the feed for ΔP = 14 bar (□ – chromium(III) retention experimental, ○ – chloride retention experimental, ---- model results)

decreases to negative value (Fig. 7b). The increase of chlorides concentration in the feed caused the increase of Cl^- ions in membrane pores and in permeate, finally. It is caused by the presence of Na^+ ions, which penetration through the membrane involves chloride ions. It means that the driving force of the permeation of chloride ions is caused by the addition of the NaCl what results in a large difference of sodium ions on both sides of the membrane. Transport of Cl^- ions depends on the type of membranes[13]. On the other hand, the retention of chromium(III) ions increased slightly as the concentration of SO_4^{2-} ions increased to level 8–10 g dm^{-3} and then achieved a plateau (Fig. 7a). Additionally, the effect of concentration polarization caused that the permeate flux significantly decreases (Fig. 8a). Similar results were obtained for different concentration of chloride ions in the feed (Fig. 8b). Morover, the average, calculated deviation for permeate flux was equal to 1.4% and 5.0%, respectively for different sulphates (Fig. 8a) and chloride (Fig. 8b) concentration in the feed.

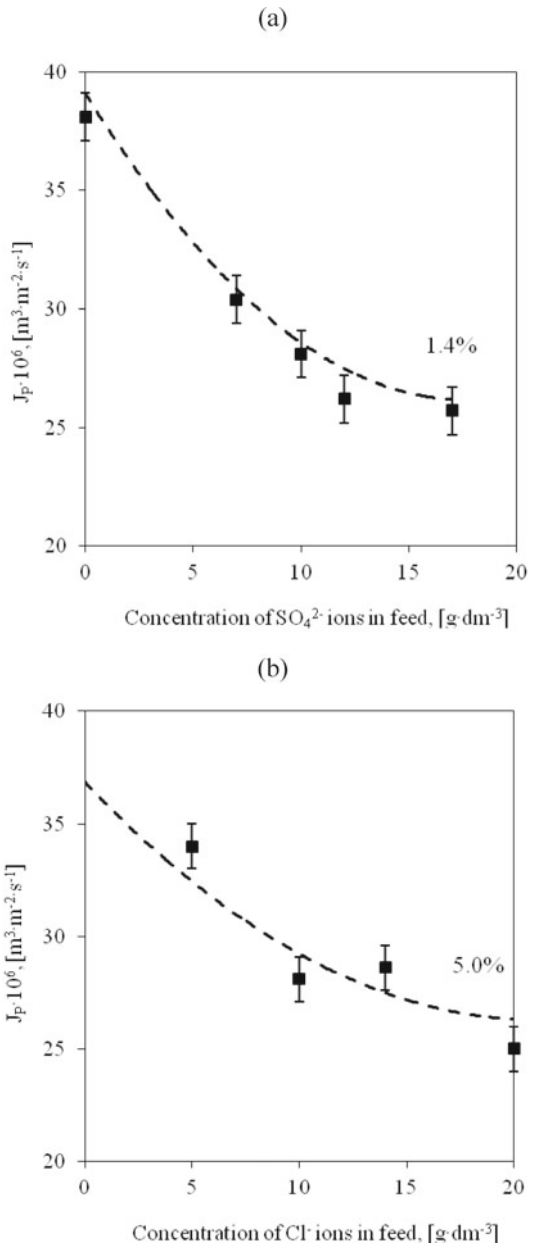

Figure 8. Permeate flux (J_P) vs. concentration of sulphate (a) and chloride (b) ions in the feed for ΔP = 14 bar (■ – experimental results, ---- model results)

CONCLUSIONS

In this paper, nanofiltration of chromium(III) salt solutions characterized by low pH were examined. The effect of pressure in the range of 10–24 bar and feed composition. characteristic for chromium tannery wastewaters, on the retention of chromium(III) and chloride ions during the nanofiltration process were analyzed. The experimental results confirmed the possibility of chromium(III) and chloride ions proper distribution between the permeate and retentate streams in the nanofiltration module. The obtained results were interpreted with DSP model which is based on extended Nernst-Planck equation and includes Donnan sferic partitioning pore and dielectric exclusion. The effect of the pore dielectric constant on the ions transport through nanofiltration membrane was analyzed by the proposed model. The obtained results allowed for derivation of the equation expressing the relationship between the pore dielectric constant and process pressure. Consequently, it was possible to obtain the satisfactory agreement between experimental and model results for different process pressure and feed composition.

ACKNOWLEDGEMENTS

This project was financed by National Science Centre granted on the basis of the decision number DEC--2013/09/N/ST8/01784.

LITERATURE CITED

1. Su, B., Wu, T., Li, Z., Cong, X., Gao, X. & Gao, C. (2015). Pilot study of seawater nanofiltration softening technology based on integrated membrane system. *Desalination* 368, 193–201. DOI: 10.1016/j.desal.2015.03.012.
2. Orecki, A., Tomaszewska, M., Karakulski, K. & Morawski, A.W. (2004). Surface water treatment by the nanofiltration method. *Desalination* 162, 47–54. DOI: 10.1016/S0011-9164(04)00026-8.
3. Liu, C., Shi, L. & Wang, R. (2015). Crosslinked layer-by-layer polyelectrolyte nanofiltration hollow fiber membrane for low-pressure water softening with the presence of SO_4^{2-} in feed water. *J. Membr. Sci.* 486, 169–176. DOI: 10.1016/j.memsci.2015.03.050.
4. Bellona, C. & Drewes, J.E. (2007). Viability of a low-pressure nanofilter in treating recycled water for water reuse applications: A pilot-scale study. *Water Res.* 41, 3948–3958. DOI: 10.1016/j.watres.2007.05.027.
5. Antczak, J., Regiec, J. & Prochaska, K. (2014). Separation and concentration of succinic acid from multicomponent aqueous solutions by nanofiltration technique. *Pol. J. Chem. Tech.* 16, 1–4. DOI: 10.2478/pjct-2014-0021.
6. Gryta, M., Markowska-Szczupak, A., Grzechulska-Damszel, J., Bastrzyk, J. & Waszak, M. (2014). The study of glycerol-based fermentation and broth downstream by nanofiltration. *Pol. J. Chem. Tech.* 16, 117–122. DOI: 10.2478/pjct-2014-0081.
7. Ortega, L.M., Lebrun, R., Noël, I.M. & Hausler, R. (2005). Application of nanofiltration in the recovery of chromium(III) from tannery effluents. *Sep. Purif. Technol.* 44, 45–52. DOI: 10.1016/j.seppur.2004.12.002.
8. Das, C., Patel, P., De, S. & DasGupta, S. (2006). Treatment of tanning effluent using nanofiltration followed by reverse osmosis. *Sep. Purif. Technol.* 50, 291–299. DOI: 10.1016/j.seppur.2005.11.034.
9. Gomes, S., Cavaco, S.A., Quina, M.J. & Gando-Ferreira, L.M. (2010). Nanofiltration process for separating Cr(III) from

acid solutions: Experimental and modelling analysis. *Desalination* 254, 80–89. DOI: 10.1016/j.desal.2009.12.010.
10. Nędzarek, A., Drost, A., Tórz, A., Harasimiuk, F. & Kwaśniewski, D. (2015). The impact of pH and sodium chloride concentration on the efficiency of the process of separating high-molecular compounds. *J. Food Proc. Engine.* 38, 115–124. DOI: 10.1111/jfpe.12131.
11. Drost, A., Nędzarek, A., Bogusławska-Wąs, E., Tórz, A. & Bonisławska, M. (2014). UF application for innovative reuse of fish brine: product quality, CCP management and the HACCP system. *J. Food Proc. Engine.* 37, 396–401. DOI: 10.1111/jfpe.12095.
12. Religa, P., Kowalik-Klimczak, A. & Gierycz, P. (2013). Study on the behavior of nanofiltration membranes using for chromium(III) recovery from salt mixture solution. *Desalination* 315, 115–123. DOI: 10.1016/j.desal.2012.10.036.
13. Religa, P., Kowalik, A. & Gierycz, P. (2011). Effect of membrane properties on chromium(III) recirculation from concentrate salt mixture solution by nanofiltration. *Desalination* 274, 164–170. DOI: 10.1016/j.desal.2011.02.006.
14. Religa, P., Kowalik, A., & Gierycz, P. (2011). A new approach to chromium concentration from salt mixture solution using nanofiltration. *Sep. Purif. Technol*. 82, 114–120. DOI: 10.1016/j.seppur.2011.08.032.
15. Tanninen, J., Mänttäri, M. & Nyström, M. (2006). Effect of salt mixture concentration on fractionation with NF membranes. *J. Membr. Sci.* 283, 57–64. DOI: 10.1016/j.memsci.2006.06.012.
16. Sharna, R.R. & Chellam, S. (2008). Solute rejection by porous thin film composite nanofiltration membranes at high feed water recoveries. *J. Coll. Inter. Sci.* 328, 353–366. DOI: 10.1016/j.jcis.2008.09.036.
17. Deon, S., Escoda, A. & Fievet, P. (2011). A transport model considering charge adsorption inside pores to describe salts rejection by nanofiltration membranes. *Chem. Eng. Sci.* 66, 2823–2832. DOI: 10.1016/j.ces.2011.03.043.
18. Deon, S., Dutournie, P., Limousy, L. & Bourseau, P. (2009). Transport of salt mixture through nanofiltration membranes: Numerical identification of electric and dielectric contributions. *Sep. Purif. Technol.* 69, 225–233. DOI: 10.1016/j.seppur.2009.07.022.
19. Chaudhari, L.B. & Murthy, Z.V.P. (2010).Separation of Cd and Ni from multicomponent aqueous solutions by nanofiltration and characterization of membrane using IT model. *J. Hazard. Mater.* 180, 309–315. DOI: 10.1016/j.jhazmat.2010.04.032.
20. Kelewou, H., Lhassani, A., Merzouki, M., Drogui, P. & Sellamuthu, B. (2011). Salts retention by nanofiltration membranes: Physicochemical and hydrodynamic approaches and modelling. *Desalination* 277, 106–112. DOI: 10.1016/j.desal.2011.04.010.
21. Jarzyńska, M. & Pietruszka, M. (2011). The application of the Kedem-Katchalsky equations to membrane transport of ethyl alcohol and glucose. *Desalination* 280, 14–19. DOI: 10.1016/j.desal.2011.07.034.
22. Schaep, J., Vandecasteele, C., Mohammad, A.W. & Bowen, W.R. (2001). Modelling the retention of ionic components for different nanofiltration membranes. *Sep. Purif. Technol*. 22–23, 169–179. DOI: 10.1016/S1383-5866(00)00163-5.
23. Mohammad, A.W. & Takriff, M.S. (2003). Predicting flux and rejection of multicomponents salts mixture in nanofiltration membranes. *Desalination* 157, 105–111. DOI: 10.1016/S0011-9164(03)00389-8.
24. Hagmeyer, G. & Gimbel, R. (1998). Modelling the salt rejection of nanofiltration membranes for ternary ion mixture and for single salts at different pH value. *Desalination* 117, 247–256. DOI: 10.1016/S0011-9164(98)00109-X.
25. Murthy, Z.V.P. & Chaudhari, L.B. (2008). Separation of binary heavy metals from aqueous solutions by nanofiltration and characterization of the membrane using Spiegler-Kedemmodel. *Chem. Eng. J.* 150, 81–187. DOI: 10.1016/j.cej.2008.12.023.
26. Nędzarek, A., Drost, A., Harasimiuk, F.B. & Tórz, A. (2015). The influence of pH and BSA on the retention of selected heavy metals in the nanofiltration process using ceramic membrane. *Desalination* 369, 62–67. DOI: 10.1016/j.desal.2015.04.019.
27. Norm PN-77/C-04604 (in Polish).
28. Norm PN-ISO 9297:1994 (in Polish).
29. Bes-Piá, A., Cuartas-Uribe, B., Mendoza-Roca, J.A. & Alcaina-Miranda, M.I. (2010). Study of the behaviour of different NF membranes for the reclamation of a secondary textile effluent in rinsing processes. *J. Hazard. Mater.* 178, 341–348. DOI: 10.1016/j.jhazmat.2010.01.085.
30. Atkins, P.W. (2012). *Physical Chemistry*. PWN.